

Fluctuations, stratification and stability in a liquid fluidized bed at low Reynolds number

This article has been downloaded from IOPscience. Please scroll down to see the full text article.

2004 J. Phys.: Condens. Matter 16 S4219

(<http://iopscience.iop.org/0953-8984/16/38/034>)

View [the table of contents for this issue](#), or go to the [journal homepage](#) for more

Download details:

IP Address: 129.252.86.83

The article was downloaded on 27/05/2010 at 17:47

Please note that [terms and conditions apply](#).

Fluctuations, stratification and stability in a liquid fluidized bed at low Reynolds number

P N Segrè^{1,3} and J P McClymer²

¹ Bio-Physics Group, NASA Marshall Space Flight Center, Huntsville, AL 35812, USA

² Department of Physics, University of Maine, Orono, ME 04469, USA

E-mail: phil.n.segre@nasa.gov

Received 6 May 2004

Published 10 September 2004

Online at stacks.iop.org/JPhysCM/16/S4219

doi:10.1088/0953-8984/16/38/034

Abstract

The sedimentation dynamics of extremely low polydispersity, non-colloidal, particles are studied in a liquid fluidized bed at low Reynolds number, $Re \ll 1$. When fluidized, the system reaches a steady state, defined where the local average volume fraction does not vary in time. In the steady state, the velocity fluctuations and the particle concentrations are found to strongly depend on height in the particle column. Using our results, we test a recently developed stability model (Segrè 2002 *Phys. Rev. Lett.* **89** 254503) for steady state sedimentation. The model describes the data well, and shows that in the steady state there is a balancing of particle fluxes due to the fluctuations and the concentration gradient. Some results are also presented for the dependence of the concentration gradient in fluidized beds on particle size; the gradients become smaller as the particles become larger and fewer in number.

1. Introduction

The sedimentation of a collection of monodisperse spheres in liquids is a fundamental problem in physics and is of wide importance in chemical reactors [2]. From numerous experiments [3–6], computer simulations [7], and theories [8–12], the following general picture has emerged. On a macroscopic scale, a collection of spheres of size D , at an average concentration ϕ_0 , settle at an average velocity $v_{\text{sed}}(\phi)$. On a microscopic, or particle scale, however, there are large non-uniformities or fluctuations in both the local concentration σ_ϕ and particle velocities σ_v . An examination of the fluctuations [4, 6] shows that the particles spontaneously organize themselves into large correlated regions, or blobs, of size $\xi \gg D$, as they settle. Significantly, it has been shown that the large scale velocity fluctuations are due to local density fluctuations. Regions where the local concentration is higher than the average fall more quickly than the

³ Author to whom any correspondence should be addressed.

average settling rate, while less dense regions fall more slowly than the average. Extensive experimental work has yielded simple scaling relations for ξ and σ_v in terms of ϕ and a [4, 5], yet a consensus on the theoretical origin or understanding of these results is still lacking.

One of the implicit assumptions in many of the experimental and theoretical works in sedimentation is that the properties of the system, including the mean concentration and fluctuation values, are uniform throughout the settling process. Recently, however, Tee *et al* [13] found that an initially uniform suspension can destabilize and become highly stratified in concentration as the particles settle. In addition, the concentration profiles continued to evolve over the entire settling time. These observations suggest that the general assumption of steady state may not always be achieved during sedimentation experiments.

To search for a state of steady state sedimentation, Segrè [1] recently conducted experiments in a liquid–solid fluidized bed. In a fluidized bed, liquid is pumped upwards through the column to counteract the force of gravity on the particles. When properly balanced, the particles are perpetually falling, and a steady state is ensured. Segrè found that all of the properties of the particle dynamics strongly depend upon the height in the particle column. A new flux balance model, relating the stratification in concentration to the fluctuations in ϕ and v , was able to explain the observed stability of the particle column.

In this paper, we expand upon this earlier work in two significant ways. First, we test whether particle size polydispersity plays a role in the observed stratification in concentration, by using particles that are much more uniform in size. The beads in this study are among the most monodisperse glass beads commercially available, with a measured size variation of $\sigma_D/D = 1.5\%$, as compared to $\sigma_D/D = 9.5\%$ in the previous work [1]. Our main finding is that a reduction in particle size polydispersity from 9.5 to 1.5% does not significantly change or remove the findings of height dependent properties and concentration stratification. Second, we examine how the stratification in concentration observed during steady state sedimentation depends upon particle size and particle number. We conduct a series of experiments on particle columns of identical heights H and average concentrations $\phi_0 = 10\%$, but with particle sizes ranging from $D = 109$ to $490 \mu\text{m}$. We find that the degree of stratification changes with particle size and particle number. The fewer the number of particles in the system, the smaller the stratification in concentration.

2. Experiment description

2.1. Particles and fluids

We use spherical glass beads, of mean diameter $D = 207 \mu\text{m}$, that have been specially filtered by the manufacturer (Mo-Sci Corp.) to be of extremely low polydispersity in size. Figure 1 shows a micrograph of a collection of the spheres. The particles lay on a flat plate and through a gentle shaking quickly organize into highly ordered forms, indicative of a low size polydispersity. To accurately determine the particle size polydispersity, we measured the variation in settling velocities of 50 individual spheres. The standard deviation of the particle settling rates is indeed extremely low, $\sigma_v/\langle v \rangle = 3.0\%$. Using the Stokes formula, $v_0 \propto \Delta\rho D^2$, and assuming the particles are all of equal density, the variation in settling rates corresponds to a variation in particle size of $\sigma_D/D = 1.5\%$.

The glass beads are dispersed in viscous solutions of glycerol and water chosen so that inertial forces during the experiments are negligible. Specifically, the particle Reynolds number is of order $Re = v_0 a \rho / \eta \approx 5 \times 10^{-3} \ll 1$. Additionally, particle motions always occur at very high Peclet numbers ($Pe \approx 10^9$), so that Brownian diffusion is negligible. The temperature is at the ambient value $T = 21 \text{ }^\circ\text{C}$.

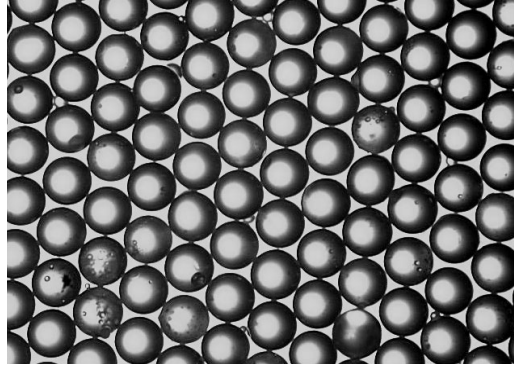


Figure 1. Micrograph of a random sampling of $D = 207 \mu\text{m}$ glass spheres.

Table 1. Particle and fluidized bed properties.

D (μm)	σ_D/D	η (cp)	v_0 (mm s^{-1})	Re	H_{bed} (cm)	$\langle\phi_{\text{bed}}\rangle$
207	0.015	27	1.21 ± 0.03	0.005	18.5	0.10

2.2. Fluidized bed

The fluidized bed consists of a fluid and particle filled glass cell through which fluid is pumped upwards to counteract the particle settling and *fluidize* the particles. The sample cell is a rectangular glass tube of dimensions $D \times W \times H = 8 \times 80 \times 305 \text{ mm}^3$. The bottom of the cell is glued into a metal base into which the water/glycerol mixture is continuously pumped. The overflow liquid at the top of the cell recirculates back into the pump, forming a closed loop. To enable a uniform flow into the cell, a 2 cm thick nylon mesh is packed with 0.5 mm diameter beads and glued across the entrance to the cell at the bottom.

With the liquid pump off, the spheres fall to the bottom of the cell and form a sediment ≈ 2.9 cm tall. When the pump is on, the particles expand upward, filling a region above the bottom up to a height dependent upon the pumped fluid velocity v_{pump} . We set the pumped fluid velocity to $v_{\text{pump}}/v_0 = 0.727 \pm 0.030$ to expand the particle column expanded to a total height $H_{\text{bed}} \sim 18.5$ cm so that the average volume fraction $\langle\phi_{\text{bed}}\rangle = 0.638(2.9/18.5) \sim 0.10$.

The main feature of a stable fluidized bed is that the average particle velocities in the laboratory frame are zero; i.e. fluid is pumped upwards at a rate that balances the particle settling rate downwards, and the particles are perpetually sedimenting.

2.3. PIV imaging system: velocity flow maps

Particle velocities are measured using the technique of particle image velocimetry (PIV) [14]. The apparatus consists of a (1008×1024 pixels) CCD camera, a synchronized stroboscope illuminating the cell from behind, and image processing hardware and software from Dantec Instruments. Velocity maps consisting of 62×62 vectors are extracted by comparing two closely timed pictures using standard PIV techniques. Each vector is the average velocity of two to four spheres.

Figure 2 shows typical velocity vector maps from a stable fluidized bed, where (a) corresponds to a position near the top and (b) to a position near the middle of the particle column. For scale, we also show the magnitude of the Stokes settling velocity v_0 . Both velocity maps show regions moving both upwards and downwards, but the magnitudes of the velocities are significantly larger near the middle than near the top.

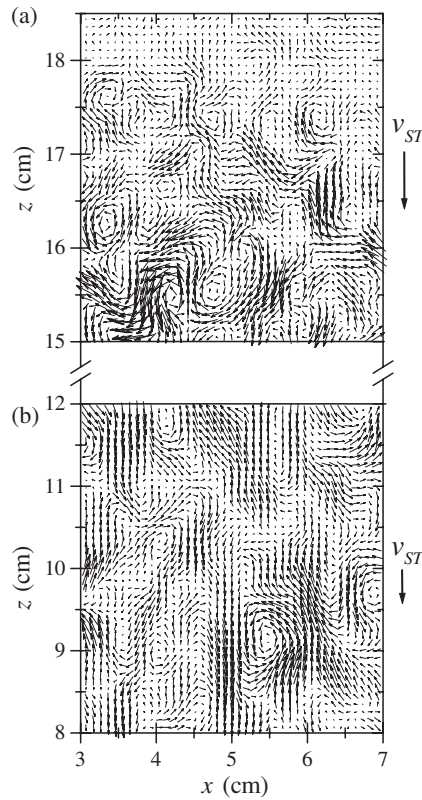


Figure 2. Velocity vector maps of a stable fluidized bed at $\langle\phi_{\text{bed}}\rangle = 0.10$. Figures (a) and (b) correspond to respective positions near the top and near the middle of the particle column. The single arrow on the right gives the corresponding scale of the Stokes settling velocity v_0 . Note that the velocity scale in (a) is magnified relative to (b) by a factor of 2 for clarity.

To quantify these observations, we measure the velocity maps and the local volume fractions at different heights along the particle column. We extract from the velocity maps the mean velocities, $v_x = \langle v_{i,x} \rangle$, and $v_z = \langle v_{i,z} \rangle$, and the root mean square (rms) velocity fluctuations, $\sigma_v^z = \langle (v_{i,z} - v_z)^2 \rangle^{1/2}$ and $\sigma_v^x = \langle (v_{i,x} - v_x)^2 \rangle^{1/2}$, where $\langle \dots \rangle$ represents an average over ~ 50 vector maps of 3844 vectors each.

2.4. Light scattering system; particle concentrations

Local particle volume fractions are determined using a laser light scattering method that measures the local optical turbidity at various heights in the particle column. To do this, we pass an expanded He–Ne laser beam, of diameter ~ 0.5 cm, through the fluidized bed at a particular height and measure the transmitted laser intensity I_T using a CCD camera. Results for a typical sample are shown in figure 3. Figure 3(a) shows the measured intensity profiles at different heights in the particle column. It is evident that the transmitted intensity varies with height, with the highest intensity at the top, and the lowest at the bottom. To find the corresponding particle concentrations, we need a calibration reference for the dependence of the transmitted intensity on particle concentration. To do this, we make several reference fluidized beds of differing average concentration ϕ_{bed} and measure the transmitted intensity

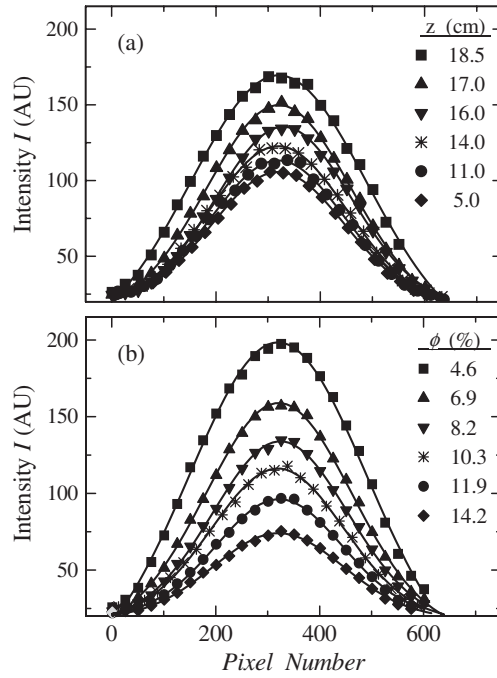


Figure 3. Measurement of local particle concentrations. (a) Transmitted laser intensity I versus height z through a fluidized bed at average volume fraction $\langle \phi \rangle = 0.10$. (b) Intensity versus ϕ calibration. Transmitted laser intensities measured at mid-height in fluidized beds of average volume fraction $0.046 \leq \langle \phi \rangle \leq 0.142$ as labelled. For clarity, only every 25th point is plotted. The solid curves are fits to Gaussian functions. The height dependent volume fraction $\phi(z)$ is extracted by comparing the $I(z)$ curve in (a) with the calibration curve $I(\phi)$ in (b).

patterns at mid-height, shown in figure 3(b). Fits of $I(z)$ and $I(\phi)$ in figures 3(a) and (b) to Gaussian functions yield peak intensity values I_{pk} . By comparing the measured values of $I_{pk}(z)$ in our fluidized bed with the reference values of $I_{pk}(\phi)$ we are able to extract the height dependent concentration $\phi(z)$ in the fluidized bed.

3. Results

3.1. Velocity fields—fluctuations

Figure 4 displays the values of the average velocities v_x and v_z , and the velocity fluctuations σ_v^x and σ_v^z for the stable fluidized bed. Measurements are taken at differing heights from near to the bottom up to the top at a height of $H_{bed} \sim 18.5$ cm. The average velocities $v_x \sim 0$ and $v_z \sim 0$, indicative of stable fluidization. The velocity fluctuations show a strong height dependence and approach zero magnitude at the top of the particle column. At all heights the level of mixing in the vertical direction is approximately twice that in the horizontal direction, i.e. $\sigma_v^z \approx 2.0\sigma_v^x$.

3.2. Velocity fields—spatial correlation lengths

The velocity vector maps, an example of which is shown in figure 2, display large regions where the velocity vectors are spatially correlated. To quantify this, we calculate several

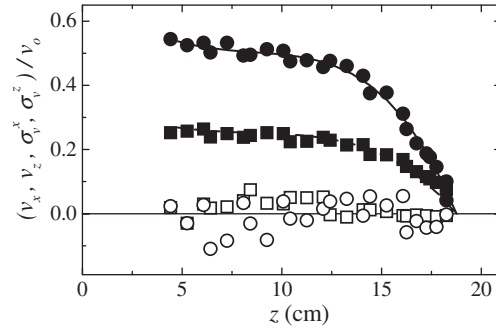


Figure 4. Normalized average velocities v_x (open squares), and v_z (open circles), and velocity fluctuations σ_v^x (closed squares), and σ_v^z (closed circles), as a function of height z . The solid lines are polynomial fits to σ_v^x , while the dashed lines are these fits divided by a constant of 2.

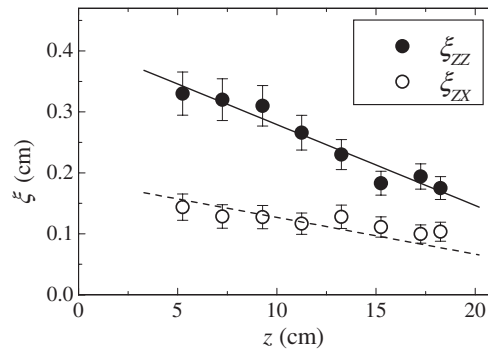


Figure 5. Correlation lengths of the velocity fluctuations in the longitudinal, ξ_{ZZ} , and transverse, ξ_{ZX} , directions. The lines are linear fits to the data.

normalized spatial correlation functions of the vertical velocity v_z . The first is a longitudinal correlation function, defined as $C_{ZZ}(z) = \langle v_z(0)v_z(z) \rangle / \langle v_z(0)^2 \rangle$, and the second is a transverse one, defined as $C_{ZX}(x) = \langle v_z(0)v_z(x) \rangle / \langle v_z(0)^2 \rangle$. Here, $\langle \dots \rangle$ represents an ensemble average over ~ 50 individual vector maps. The correlation functions fit well to the forms $C_{ZZ}(z) = \exp(-z/\xi_{ZZ})$ and $C_{ZX}(z) = \exp(-z/\xi_{ZX})$, allowing us to extract ξ_{ZZ} and ξ_{ZX} , the characteristic longitudinal and transverse correlation lengths of the velocity fluctuations. Results for ξ_{ZZ} and ξ_{ZX} are shown in figure 5. The correlation lengths are not uniform in height, and exhibit a monotonic decrease towards the top part of the column [1].

3.3. Concentration profiles

To examine the concentration profiles, and in particular look for the presence or absence of a vertical density stratification, we use the laser scattering method described in section 2.4 above. This technique allows for highly accurate determinations of the local particle volume fraction $\phi(z)$ as a function of height z .

In figure 6 we show results for the local particle volume fraction $\phi(z)$ as a function of height z . There is a marked stratification in concentration with height; the concentration is significantly greater at the bottom than at the top. Note also the sharp interface at the top, with ϕ dropping from the values $\phi \sim 0.06$ to $\phi \sim 0.00$ within ~ 0.5 cm. While most of the concentration variation occurs in the highest portions of the particle column, measurable and

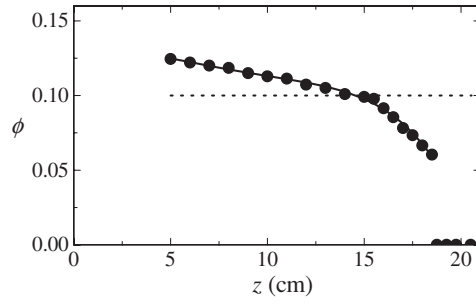


Figure 6. Particle volume fraction ϕ as a function of height z . The dashed line represents the mean particle concentration, $\phi = 0.10$.

Table 2. Measured properties of the fluidized bed described in table 1. D is the particle diameter and N_{tot} the total number of particles fluidized. v_{pump}/v_0 is the normalized fluidizing pump velocity upwards. $v_{\text{top}}^{\text{sed}}/v_0$ is the initial sedimentation velocity of the top interface, measured just after the fluid pump is turned off. ϕ_{top} is the particle concentration (%) measured just below the top interface. The particle concentrations $\phi_{\text{top}}^{\text{pump}}$ and $\phi_{\text{top}}^{\text{sed}}$ are calculated from v_{pump}/v_0 and v_{sed}/v_0 using the Richardson–Zaki equation $v/v_0 = (1 - \phi)^{5.5}$.

D (μm)	N_{tot}	v_{pump}/v_0	$v_{\text{top}}^{\text{sed}}/v_0$	ϕ_{top}	ϕ_{pump}	$\phi_{\text{top}}^{\text{sed}}$
207	2.7×10^6	0.727 ± 0.030	0.686 ± 0.030	6.0 ± 0.3	5.6 ± 0.7	6.6 ± 0.7

significant gradients occur at all heights. For convenience, we refer to the concentration value at the closest measured point to the top interface as ϕ_{top} , and we find $\phi_{\text{top}} = 6.0 \pm 0.3\%$.

3.4. Particle sedimentation and fluid pump velocities

The stratification in concentration seen in figure 6 can help explain the value of the normalized fluid pump velocity v_{pump}/v_0 , listed in table 2. If the particle column were perfectly uniform in concentration at the average value $\phi_0 = 0.10$, one would then expect that the upward fluid velocity needed to achieve stable fluidization would be equal and opposite to the sedimentation velocity at volume fraction ϕ_0 , i.e. $v_{\text{pump}}/v_0 = -v_{\text{sed}}(\phi_0)/v_0$. To test this, we take advantage of the well known equation for the sedimentation velocity of a collection of spheres at volume fraction ϕ , the Richardson–Zaki (RZ) equation [15], $v_{\text{sed}}(\phi)/v_0 = (1 - \phi)^{5.5}$. This equation allows us to calculate the sedimentation velocity at average concentration $\phi = 0.10$, the value being $v_{\text{sed}}(\phi = 0.10)/v_0 = 0.56$. As seen in table 2, this value is more than 20% smaller than the measured pump velocity, $v_{\text{pump}}/v_0 = 0.727 \pm 0.030$. In essence, the velocity of the fluid pumped upwards is *greater* than the average particle sedimentation velocity downwards. The net result, which will be an important component of how fluidized beds stabilize themselves against large fluctuations as discussed in section 4, is that the particles are being pushed upwards at all times by this mismatch in sedimentation and pump velocities.

If the fluid pump velocity does not match the calculated sedimentation velocity at $\phi = 0.10$, then one can ask to what concentration ϕ corresponds the value v_{pump} ? To answer this, we use the value of measured values v_{pump}/v_0 and the RZ equation to calculate $\phi_{\text{pump}} = 1 - (v_{\text{pump}}/v_0)^{1/5.5}$; we find $\phi_{\text{pump}} = 5.6 \pm 0.7\%$. Significantly, this value is very similar to the measured concentration at the top of the particle column, $\phi_{\text{top}} \simeq 6.0 \pm 0.3\%$.

To gain a global perspective of the local settling rates throughout the particle column, we plot in figure 7 the calculated sedimentation velocities $v_{\text{sed}}(\phi(z))/v_0 = (1 - \phi(z))^{5.5}$ from the

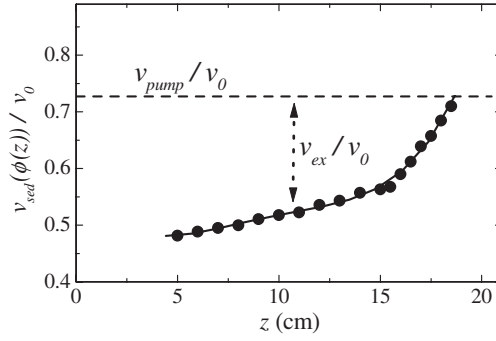


Figure 7. Particle sedimentation velocities v_{sed}/v_0 , calculated using the height dependent volume fractions $\phi(z)$ in figure 6 and the Richardson–Zaki equation $v_{\text{sed}}/v_0 = (1 - \phi)^{5.5}$, as a function of height z . The dashed line represents the value of the normalized fluid pump velocity, v_{pump}/v_0 , used to stabilize the particle column.

height dependent concentration profiles $\phi(z)$ shown in figure 6. Also indicated by the dashed line is the fluid pump velocity used to achieve stable fluidization. The value of v_{pump}/v_0 closely matches the settling rate at the top of the column, but is significantly greater than v_{sed}/v_0 at all other heights. The net difference between the fluid velocity pumped upwards and the settling velocity downwards is defined as the excess velocity $v_{\text{ex}}/v_0 = [v_{\text{pump}} - v_{\text{sed}}(z)]/v_0$.

4. Stability analysis

The results presented above give a rather complete characterization of the concentration profiles and particle velocity dynamics in a stable fluidized bed consisting of extremely low polydispersity spheres ($\sigma_D/D = 1.5\%$). We find that all of the properties measured display marked dependences on height in the particle column. A fluidized bed can be thought of as a system where the particles are sedimenting *perpetually*. The results for the *rms* velocity fluctuations and the concentration profiles are stable in time and represent the steady state behaviour of the system. The finding of steady state behaviour has important implications which we can exploit to help understand the concentration and fluctuation profiles observed during fluidization. In section 4.1 we describe the criterion for fluidized bed stability in terms of a general flux balance relation. In sections 4.1.1, 4.1.2 and 4.2 we evaluate and test this stability criterion using the recently developed model of Segrè [1].

4.1. General condition for fluidized bed stability

In the steady state the average volume fraction at all points in the particle column is constant in time, i.e. $\partial\phi(z)/\partial t = 0$. This condition can be written in terms of particle fluxes using the conservation of mass, or continuity, equation $\partial\phi(z)/\partial t = -\nabla \cdot \mathbf{j}(\mathbf{z}) = 0$ [15], where $\mathbf{j}(\mathbf{z}) = \phi(z)\mathbf{v}(\mathbf{z})$, and $\mathbf{v}(\mathbf{z})$ is a locally coarse grained velocity. To account for the fluctuations in the system, we expand the particle flux to first order, $\mathbf{j}(\mathbf{z}) = \mathbf{j}_0(\mathbf{z}) + \delta\mathbf{j}(\mathbf{z})$, and assuming $\partial j_x/\partial x = \partial j_y/\partial y = 0$, and $j(z) = j_z(z)$, the continuity equation yields a requirement that gradients in the local particle fluxes sum to zero, i.e.

$$\frac{\partial j_0(z)}{\partial z} = -\frac{\partial \delta j(z)}{\partial z}. \quad (1)$$

This stability condition can be integrated to yield

$$j_0(z) = -\int_z^H dz' \left[\frac{\partial \delta j(z')}{\partial z'} \right], \quad (2)$$

where we have left the fluctuation term in an integral form which will be easier for direct evaluation as described below.

The stability criterion equation (2) can be expressed directly in terms of the quantities measured, the particle concentration and velocity fields, by expanding $\phi(z) \rightarrow \phi_0(z) + \delta\phi(z)$ and $v(z) \rightarrow v_0(z) + \delta v(z)$, yielding for the zeroth order particle flux (the lhs of equation (2)),

$$j_0(z) = \langle \phi_0(z)v_0(z) \rangle, \quad (3)$$

and for the particle flux due to fluctuations (the rhs of equation (2)),

$$\delta j(z) = \langle \phi_0(z)\delta v(z) + \delta\phi(z)v_0(z) + \delta\phi(z)\delta v(z) \rangle, \quad (4)$$

where $\langle \dots \rangle$ represents an ensemble average at each height.

The stability criterion, equation (2), expresses the general relationship that must exist for a particle fluidized bed to be stable. To evaluate and test this criterion on our data we need to develop expressions for $j_0(z)$ and $\delta j(z)$ in terms of the measured quantities, and we follow closely below the development from Segrè [1].

4.1.1. Particle flux due to the stratification in concentration. The zeroth order particle flux, $j_0(z) = \langle \phi_0(z)v_0(z) \rangle$, is found from the difference between the mean upward flux due to the pump flow, $j_{\text{pump}}(z) = +\phi(z)v_{\text{pump}}$, and the mean downward flux due to sedimentation, $j_{\text{sed}}(z) = -\phi(z)v_{\text{sed}}(z)$. The net flux is given by the difference

$$j_0(z) = \phi(z)v_{\text{ex}}(z) = \phi(z)[v_{\text{pump}} - v_{\text{sed}}(z)], \quad (5)$$

where we define the excess velocity as $v_{\text{ex}}(z) \equiv v_{\text{pump}} - v_{\text{sed}}(z)$. The height dependent sedimentation velocities $v_{\text{sed}}(z)$, shown in figure 7, are calculated from the concentration profiles $\phi(z)$ and the RZ equation. At the top of the column, $v_{\text{sed}}(z)$ and v_{pump} are nearly equal, but at all other positions the upward fluid velocity is greater than the downward sedimentation velocities, i.e. $v_{\text{pump}} > v_{\text{sed}}(z)$, resulting in a net particle flux upwards.

4.1.2. Particle flux due to velocity and concentration fluctuations. The general relation for the particle flux due to fluctuations, equation (4), is expressed in terms of the fluctuations in velocity and volume fraction. The first two terms are zero because $\langle \delta v(z) \rangle = 0$ and $\langle \delta\phi(z) \rangle = 0$. The product $\langle \delta\phi\delta v \rangle$ is non-zero because fluctuations in volume fraction and velocity are correlated [6]. The more concentrated regions move downwards, $(+\delta\phi)(-\delta v)$, and the less concentrated regions move upwards, $(-\delta\phi)(+\delta v)$, so that $\delta j(z) < 0$ and fluctuations result in a net particle flux *downwards*. To estimate $\delta\phi$, we use a simple model based upon random statistics [2]. Fluctuations occur in regions of linear size ξ , and contain on average $N_\xi = \phi\xi^3/a^3$ particles, assuming that the particles are randomly distributed. The rms fluctuations are determined as $\sigma_{N_\xi} = \sqrt{N_\xi S(\phi)}$, where $S(\phi)$ accounts for excluded volume effects and is calculated from the Carnahan–Starling equation for hard spheres [15]. The rms fluctuations in volume fraction are then $\sigma_\phi = \sigma_{N_\xi} (a/\xi)^3 = \sqrt{\phi S(\phi) a^3/\xi^3}$.

Approximating the values of $\delta\phi \rightarrow \sigma_\phi$ and $\delta v \rightarrow \sigma_v^z$, and replacing the derivative term as $\partial/\partial z \rightarrow C_\xi/\xi$, where C_ξ is an adjustable constant expected to be of order unity, the flux due to fluctuations is

$$\partial[\delta j(z)]/\partial z \simeq -C_\xi \sigma_\phi \sigma_v^z / \xi, \quad (6)$$

which can be written out in terms of the measured quantities using the expression for σ_ϕ as

$$\partial[\delta j(z)]/\partial z = -C_\xi \sigma_v^z(z) \sqrt{S(\phi)\phi(z)a^3/\xi(z)^5}. \quad (7)$$

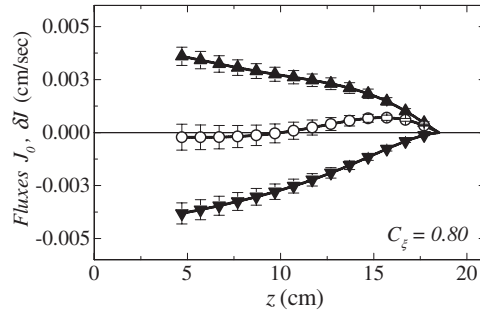


Figure 8. Stability test: particle fluxes $j_0(z)$ (up triangle), from equation (5), and $\delta j(z)$ (down triangle), from equation (8), and their sum $j_0(z) + \delta j(z)$ (\circ) as a function of height z in a stable fluidized bed. With the constant $c_\xi = 0.80$ the particle fluxes sum to near zero at all heights, indicative of a stable steady state particle column.

The negative values of $\delta j(z)$ indicate that the coupling of velocity and concentration fluctuations results in a net flux of particles downwards. The particle flux due to fluctuations, the rhs of equation (2), is then

$$\delta j(z) = -C_\xi \int_z^H \sigma_v^z(z') \sqrt{\frac{S(\phi)\phi(z')a^3}{\xi(z')^5}} dz'. \quad (8)$$

4.2. Test of criterion for fluidized bed stability

We now explicitly test the stability condition, equation (2), using the expressions for $j_0(z)$ and $\delta j(z)$ in equations (5) and (8). All of the variables needed to evaluate equations (5) and (8), with the exception of $v_{\text{sed}}(z)$, were directly measured. The sedimentation velocities $v_{\text{sed}}(z)$ were calculated from our data for $\phi(z)$ using the RZ equation [15]. Polynomial fits to our data for $\phi(z)$, $\xi(z)$ and $\sigma_v^z(z)$ were used in the evaluation.

The results for the particle fluxes due to the concentration stratification, $j_0(z)$, the velocity and concentration fluctuations, $\delta j(z)$, and their sum, $j_0(z) + \delta j(z)$, are shown in figure 8. The values for $j_0(z)$ indicate near zero net flux at the top of the bed, due to the matching of the pumped fluid and particle sedimentation velocities, and *positive* and increasing fluxes towards the lower part of the bed where the pumped fluid velocities are greater than the local sedimentation rates. At the top of the column $\delta j(z)$ also vanishes due to the vanishing of the velocity fluctuations, while *negative* and increasing fluxes are found towards the lower part of the bed where the fluctuations in $\sigma_v^z(z)$ and $\sigma_\phi(z)$ become larger.

Strikingly, the net particle flux, obtained from summing the integrals of the two flux gradient terms, i.e. $j_0(z)$ and $\delta j(z)$ together, is near zero over the entire height of the column. These results show that the particle column is stable because the particle flux downward due to fluctuations is nearly equal and opposite to the flux upwards due to the stratification in ϕv_{ex} . The equality of the flux gradients leads to the stability relation, expressed in derivative form,

$$\frac{\partial[\phi(z)v_{\text{ex}}(z)]}{\partial z} = -C_\xi \sigma_v^z(z) \sqrt{\frac{S(\phi)\phi(z)a^3}{\xi(z)^5}}, \quad (9)$$

which shows that the magnitudes of the fluctuations are related to the degree of stratification.

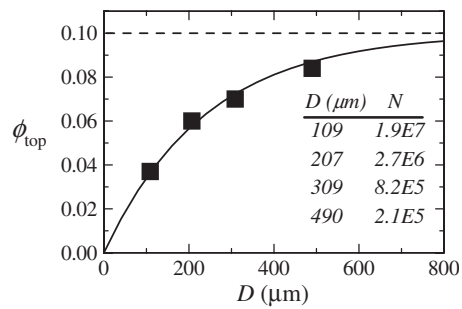


Figure 9. Measured volume fraction at the top of the particle columns, ϕ_{top} , as a function of particle diameter D . The solid curve is a guide to the eye. The dashed line represents the mean concentration in all the beds, $\phi_0 = 0.10$, and N is the total number of particles in each fluidized bed.

4.3. Fluidized beds with varying particle sizes

The results above show that a strong stratification in concentration is present during fluidization; the concentration at the top of the particle column is significantly lower than the mean. How does this stratification vary with particle size or the number of particles in the system? To answer this, we examine a series of four fluidized beds with identical mean concentrations, $\phi_0 = 0.10$, identical particle column heights, $H \approx 18.5$ cm, but differing particle sizes, with $D = 109, 207, 309,$ and $490 \mu\text{m}$. While a full accounting of these experiments is in preparation [16], we show in figure 9 measured values of the volume fraction just below the top interface, ϕ_{top} . The degree of stratification changes with particle size. For the largest particles, $D = 490 \mu\text{m}$, the difference of the top from the mean ($\phi = 0.10$) is only $\Delta\phi = (0.10 - \phi_{\text{top}}) \sim 0.016$. With decreasing particle size this value increases significantly, equaling $\Delta\phi \sim 0.063$ for the smallest particles. In terms of the total number of particles N fluidized, the system becomes more uniform as N decreases.

5. Conclusions

The sedimentation dynamics of non-colloidal spheres were studied in a liquid fluidized bed at low Reynolds number. The spheres were of much higher uniformity in size than those used in prior studies [1]. During fluidization, the system reached a steady state, defined where the local average volume fraction does not vary in time. In steady state, the velocity fluctuations and the particle concentrations were found to strongly depend on height in the particle column. Using our results, we tested a recently developed stability model [1] for steady state sedimentation. The model describes our data well, and shows that in the steady state there is a balancing of particle fluxes due to the fluctuations and the concentration gradient. Some results are also presented for the dependence of the concentration gradient in fluidized beds on particle size; the gradients become smaller as the particles become larger and fewer in number. The large question that remains as yet unanswered is what controls the degree of particle stratification or the fluctuation magnitudes. The stability model connects together these two quantities, but cannot *a priori* predict either of their values in the absence of knowledge of the other.

Acknowledgments

We thank Shang Tee and Tony Ladd for discussions, in particular for stressing the importance of using nearly monodisperse beads.

References

- [1] Segrè P N 2002 *Phys. Rev. Lett.* **89** 254503
- [2] Hinch E J 1988 *Disorder in Mixing* ed E Guyon *et al* (Dordrecht: Kluwer–Academic) p 153
- [3] Nicolai H and Guazzelli E 1995 *Phys. Fluids* **7** 3
Nicolai H, Herzhaft B, Hinch E J, Oger L and Guazzelli E 1995 *Phys. Fluids* **7** 12
- [4] Segrè P N, Herbolzheimer E and Chaikin P M 1997 *Phys. Rev. Lett.* **79** 2574
- [5] Segrè P N, Liu F, Umbanhower P and Weitz D A 2001 *Nature* **409** 594
- [6] Lei X, Ackerson B J and Tong P 2001 *Phys. Rev. Lett.* **86** 3300
- [7] Ladd A J C 1996 *Phys. Rev. Lett.* **76** 1392
Ladd A J C 2002 *Phys. Rev. Lett.* **88** 48301
- [8] Caffisch R E and Luke J H C 1985 *Phys. Fluids* **28** 259
- [9] Koch D L and Shaqfeh E S G 1991 *J. Fluid Mech.* **224** 275
- [10] Levine A, Ramaswamy S, Frey E and Bruinsma R 1998 *Phys. Rev. Lett.* **81** 5944
- [11] Tong P and Ackerson B J 1998 *Phys. Rev. E* **58** 6931
- [12] Brenner M P 1999 *Phys. Fluids* **11** 754
- [13] Tee S Y, Mucha P J, Cipelletti L, Manley S, Brenner M P, Segrè P N and Weitz D A 2002 *Phys. Rev. Lett.* **89** 54501
- [14] Adrian R J 1991 *Annu. Rev. Fluid Mech.* **23** 261
- [15] Russel W B, Saville D A and Schowalter W R 1989 *Colloidal Dispersions* (Cambridge: Cambridge University Press)
- [16] Segrè P N and McClymer J P 2004 in preparation